Proceedings of the Research Institute of Atmospherics,
Nagoya University, vol.35(1988)

RESEARCH REPORT

A COMPUTER MODEL OF THE EARTH'S MAGNETOSPHERE

Tatsuki Ogino, Raymond J. Walker[1],
and Maha Ashour-Abdalla[1,2]

[1] Institute of Geophysics and Planetary Physics, University of California, Los Angeles, California 90024, U.S.A.
[2] Department of Physics, University of California, Los Angeles, California 90024, U.S.A.

Abstract

The dependence of the magnetospheric configuration and polar cap structure on the north-south component of the interplanetary magnetic field (IMF) has been modeled by performing a three-dimensional time-dependent magnetohydrodynamic (MHD) simulation of the interaction between the solar wind and the earth's magnetosphere. When a uniform southward IMF (B_z=-5nT) is initially imposed throughout the system, magnetic neutral lines are formed in the subsolar and midnight tail regions on the equator. The magnetic field lines are dipolar near the earth and very concave in the magnetotail. The plasma convection is antisunward near the noon-midnight meridian and the plasma sheet becomes extremely thin. When the southward IMF begins to flow into the simulation box with the solar wind it takes more than about 40 minutes until tail magnetic reconnection begins. For no IMF, the dayside magnetic reconnection stops.

When a uniform northward IMF (B_z=5nT) is initially imposed throughout the system, the plasma sheet thickens in a small region near the noon-midnight meridian and extends into the tail lobes. When viewed from the polar cap, this appears as a narrow finger of closed field lines extending into the polar cap. The plasma sheet extension becomes less pronounced when the northward IMF begins to enter the simulation box with the solar wind. For both cases the convection near

the noon-midnight meridian is sunward, and field aligned currents of the region 1 type appear on both sides of the plasma sheet extension. When the IMF is southward, the polar cap expands until it reaches 65° latitude at midnight while it shrinks to 80° for northward IMF.

1. Introduction

It is not easy to understand the interaction process between the solar wind and a planetary magnetosphere from only the limited measurements provided by a spacecraft. This is because the observations are temporarily and spatially limited to the spacecraft trajectory. In order to understand a magnetospheric system, the experimentalist is challenged to interpret the limited single point measurements in terms of a large-scale and highly dynamic system. During the past several years a new technique, computer simulation by using the global magnetohydrodynamic (MHD) model, has been developed to solve the magnetospheric configuration and to present a self-consistent picture of the solar wind-magnetosphere interaction process.

The first global MHD simulation of the earth's magnetosphere was presented by Leboeuf et al. [1978]. They used a 2-dimensional particle MHD code to produce a magnetospheric topology consistent with Dungey's reconnection model for a southward interplanetary magnetic field (IMF). Leboeuf et al. [1981] successfully extended their 2-dimensional code to a 3-dimensional code, and again reproduced a similar topology. Leboeuf et al. used MHD particle code. The MHD particle code has the advantage of being numerically stable in regions with very low plasma density where the local Alfven speed is high without the small time steps required for other methods. However, the plasma sheet was short (about -30 R_e) because of the large numerical magnetic diffusion in the code. The 2-dimensional interaction between the solar wind and the earth's magnetosphere was simulated by using a minimally diffusive MHD code by Lyon et al. [1980]. Their results showed the basic features of the magnetosphere such as bow shock, magnetopause and a long magnetotail. They used flux-corrected transport (FCT) for the hydrodynamic variables and the partial donor cell method (PDM) for the magnetic field. Lyon et al. [1981; 1986] modified the MHD code and used it to simulate a substorm-like process occurring in the earth's magnetosphere. They employed a leapfrog time-integration scheme, a 20th-order finite difference approximation

for the spatial derivatives and flux-corrected transport. This MHD code produced a long magnetotail (more than -60R_e) and obtained the results consistent with the near-earth magnetic neutral-line model of substorms.

Brecht et al. [1981; 1982] developed a 3-dimensional version in which the partial donor cell method was used on an inhomogeneous grid. As a result they could successfully treat a longer magnetotail (-90R_e) as well as the sharp gradients of the bow shock and the magnetopause in the dayside interaction region. Wu et al. [1981] simulated the steady state magnetospheric configuration to reproduce many of the magnetospheric features such as bow shock, magnetopause and plasma sheet at quiet times by using a 3-dimensional MHD model, in which the Rusanov numerical scheme was used. Wu applied the MHD model to study the shape of the magnetosphere [Wu, 1983] and the effect of dipole tilt on the magnetospheric structure [Wu, 1984].

The interaction of the solar wind with the earth's magnetosphere was also studied by using a different time-dependent 3-dimensional MHD model by Ogino and co-workers [Ogino, 1986; Ogino and Walker, 1984; Ogino et al., 1985; 1986], where a modified two step Lax-Wendroff scheme was adopted. They projected the physical quantities such as the parallel vorticity and field aligned currents onto the polar cap along magnetic field lines in order to compare the simulation results with observations and demonstrated that the projected patterns of the magnetospheric convection system and field aligned currents depended strongly on the IMF orientation. In general the model reproduced well the observed ions from polar orbiting satellites [Walker and Ogino, 1987]. The nature of the solar wind-magnetosphere-ionosphere coupling was also simulated by Fedder and Lyon [1987] in order to investigate the physics and behavior of the controlling processes. They showed that the current-voltage relationship in the magnetosphere was a dynamo process and discussed the operation of the dynamo and its location.

The main purpose of the present paper is to study the role of the north-south component of the IMF on the earth's magnetospheric configuration and polar cap structure by using a three-dimensional time-dependent MHD model with a high spatial resolution of 0.5Re grid spacing. The simulation results for five typical cases with different IMF conditions will be presented and discussed in terms of the magnetospheric convection, field aligned currents and polar cap size.

2. Simulation Model

We will only briefly review the simulation model here, because it has been described in detail elsewhere [Ogino, 1986; Ogino et al., 1985]. The present purpose is to study the effects of the north-south component of the IMF on the magnetospheric configuration by using a 3-dimensional global MHD simulation. Therefore, we have solved the MHD and Maxwell's equations in the northern and dusk quarter (Figure 1) as an initial value problem by using the modified two step Lax-Wendroff scheme. The normalized MHD equations are written as follows,

$$\frac{\partial \rho}{\partial t} = -\vec{\nabla} \cdot (\vec{v}\rho) + D\nabla^2\rho \tag{1a}$$

$$\frac{\partial \vec{v}}{\partial t} = -(\vec{v} \cdot \vec{\nabla})\vec{v} - \frac{1}{\rho}\vec{\nabla}p + \frac{1}{\rho}\vec{J} \times \vec{B} + \vec{g} + \frac{1}{\rho}\vec{\Phi} \tag{1b}$$

$$\frac{\partial p}{\partial t} = -(\vec{v} \cdot \vec{\nabla})p - \Gamma p\vec{\nabla} \cdot \vec{v} + D_p\nabla^2 p \tag{1c}$$

$$\frac{\partial \vec{B}}{\partial t} = \vec{\nabla} \times (\vec{v} \times \vec{B}) - \eta\nabla^2\vec{B} \tag{1d}$$

$$\vec{J} = \vec{\nabla} \times (\vec{B} - \vec{B}_d), \tag{1e}$$

where ρ is the plasma density, $\vec{v}$ the flow velocity, p the plasma pressure, $\vec{B}$ the magnetic field, $\vec{B}_d$ the dipole field, $\vec{J}$ the current density, $\vec{g}$ the gravitational force, $\vec{\Phi} \equiv \mu\nabla^2\vec{v}$ the viscosity, $\Gamma = 5/3$ the ratio of the specific heats, $\eta = \eta_o(T/T_o)^{-3/2}$ the resistivity and T/T_o is the temperature normalized by its value in the ionosphere. The units for distance, velocity, and time are the earth's radius, R_e = 6.37 x 10^6m, the Alfven speed at one earth radius on the equator, v_A = 6.80 x 10^6m/s and the Alfven transit time, $t_A = Re/v_A$ = 0.937s. The numerical coefficients are η_o = 0.002, $\mu/\rho_{sw} = D = D_p$ = 0.001 where ρ_{sw} is the solar wind density. The values of μ, D and D_p were chosen to be small enough that they would not have significant influence on the global magnetospheric structure and yet be large enough to suppress numerical fluctuations which otherwise occur with a scale of one grid space. The magnetic Reynold's number, which is the magnetic diffusion time divided by the Alfven transit time, is S = 200 - 2000. It is small near the earth and becomes larger in the distant magnetosphere.

The solar magnetospheric coordinate system shown in Figure 1 was used in the calculation. A uniform solar wind with $n_{sw} = 5/cm^3$, $v_{sw} = 300$ km/s and $T_{sw} = 2 \times 10^5$ °K flows into a simulation box of dimensions, $x_o \leq x \leq x_1$, $0 \leq y \leq y_o$ and $0 \leq z \leq z_o$ at $x = x_1$, where typically $x_o = -50.25R_e$, $x_1 = y_o = z_o = 25.25R_e$. Free boundary conditions, where the derivatives of all physical quantities are zero, were used at $x = x_o$, $y = y_o$ and $z = z_o$. Mirror boundary conditions were used at $y = 0$ and $z=0$. At the mirror boundary at $y=0$, $\psi(-y, z) = \psi(y, z)$ is satisfied for ρ, v_x, v_z, p, B_x and B_z and $\psi(-y, z) = -\psi(y, z)$ is satisfied for v_y and B_y. At $z=0$, $\psi(y, -z) = \psi(y, z)$ is satisfied for ρ, v_x, v_y, p and B_z and $\psi(y, z) = -\psi(y, z)$ is satisfied for v_z, B_x and B_y. Simple ionospheric boundary conditions were imposed near the earth. At the ionosphere a static equilibrium was maintained [Ogino, 1986], in which all the parameters are held constant for $\xi \equiv (x^2 + y^2 + z^2)^{1/2} < 3.5R_e$ and all perturbations are damped out by using a smoothing function near the ionosphere ($\xi \leq 5.5R_e$). Therefore, the field aligned currents also disappear near the earth and do not form a closed loop in the ionosphere. Instead, they close in the magnetosphere. The MHD equations were solved on a $(N_x, N_y, N_z) = (150, 50, 50)$ point grid exclusive of the boundary grid points. The mesh size was $\Delta x = \Delta y = \Delta z = 0.5R_e$ and the time step, Δt, was selected as $4\Delta x/v_A = 1.87$s in order to assure that the numerical stability criterion, $v_g^{max}\, \Delta t/\Delta x < 1$, where v_g^{max} is the maximum group velocity in the calculation domain, was met.

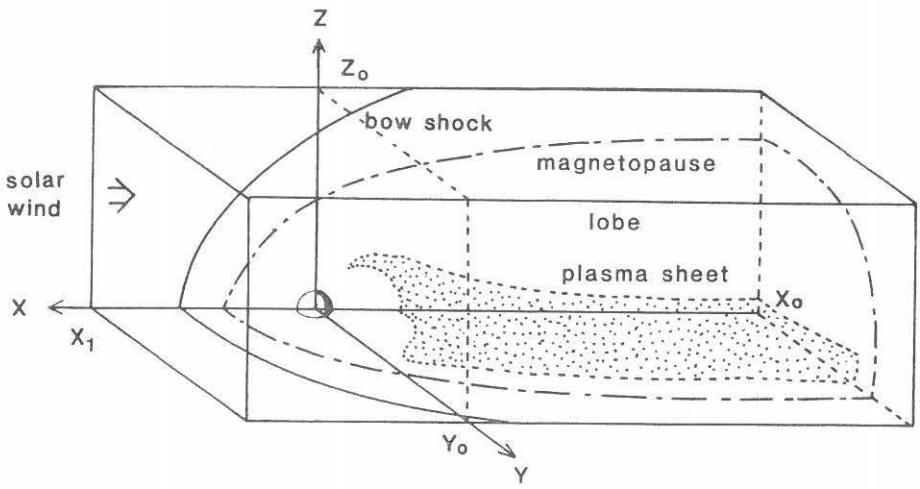

Fig. 1. Solar-magnetospheric coordinate system for the three-dimensional global MHD simulation.

3. Simulation Results

The response of the magnetospheric configuration and the polar cap structure to the north-south component of the IMF will be demonstrated in this section. In each case, a snap shot of the quasi-steady state magnetospheric configuration has been shown. The quasi-steady state was determined by running the code until the large scale structure of the magnetosphere stopped changing. Some of the small-scale structure of the plasma sheet continue to evolve up until the ends of the simulation runs.

3.1 Simulation result for low spatial resolution

To start this study, we first ran the high resolution code with the same parameters used in our previous simulation results [Ogino and Walker, 1984; Ogino et al., 1985; 1986]. We employed the same grid $(N_x, N_y, N_z) = (60, 30, 30)$ and the same grid spacing of $\Delta x = \Delta y = \Delta z$

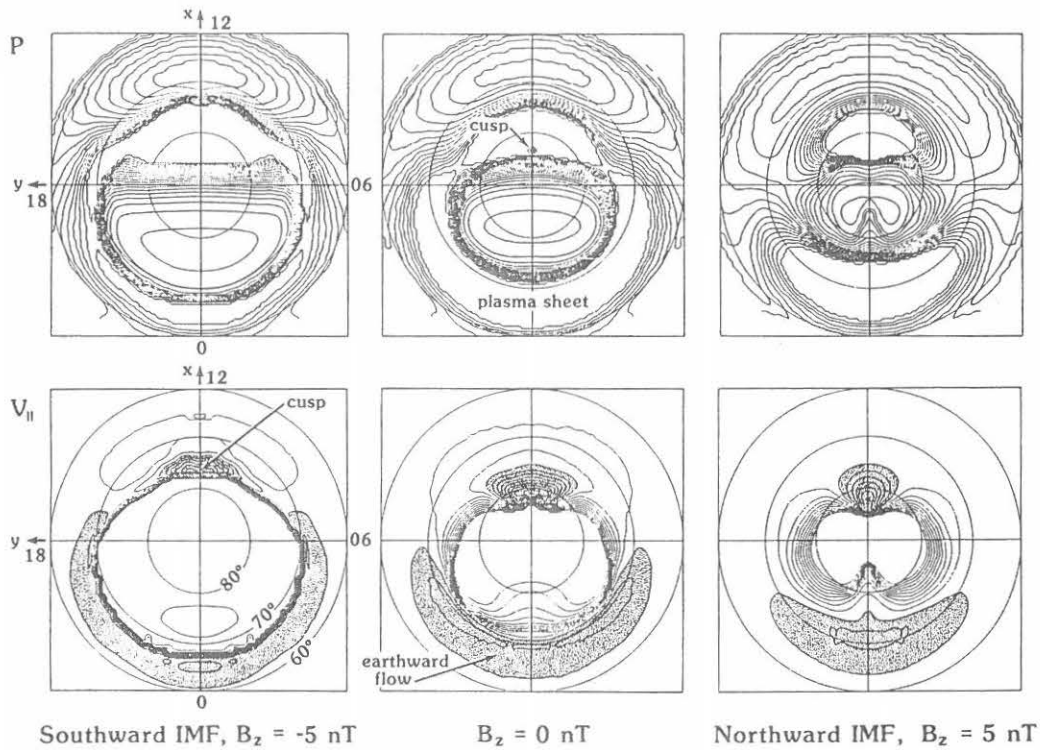

Fig. 2. Northern polar projections of the plasma pressure, p and the parallel velocity, $v_{\parallel}$ for southward IMF (B_z=-5nT), no IMF (B_z=0nT) and northward IMF (B_z=5nT). The hatched areas correspond to earthward flow.

$= 1R_e$.

In Figure 2 we have plotted northern polar projections of the plasma pressure, p and the parallel velocity, $v_{\parallel}$ for three different IMF conditions. The hatched areas correspond to the earthward flow for $v_{\parallel}$. The snap shot was taken at 512 time steps or 32 minutes after the beginning of the simulation. The southward or northward IMF was initially imposed throughout the system. The plasma parameters for p and $v_{\parallel}$ in Figure 2 have been projected along magnetic field lines into the northern hemisphere of the earth. The projected values were determined by calculating $\int(f/B)dl/\int(1/B)dl$ along the magnetic field lines in the simulation box where f stands for each of the plasma parameters and B is the field magnitude. The expression generally gives an averaged value in the magnetic flux tube, and the projected angle, which corresponds to an interval of Δx at a distance of ξ from the earth, is approximately calculated by $\theta = (180/\pi)(\xi/R_e)^{-3/2}(\Delta x/R_e)$ degrees near the pole. On the northern polar plots the positions of the dayside cusp and the plasma sheet can

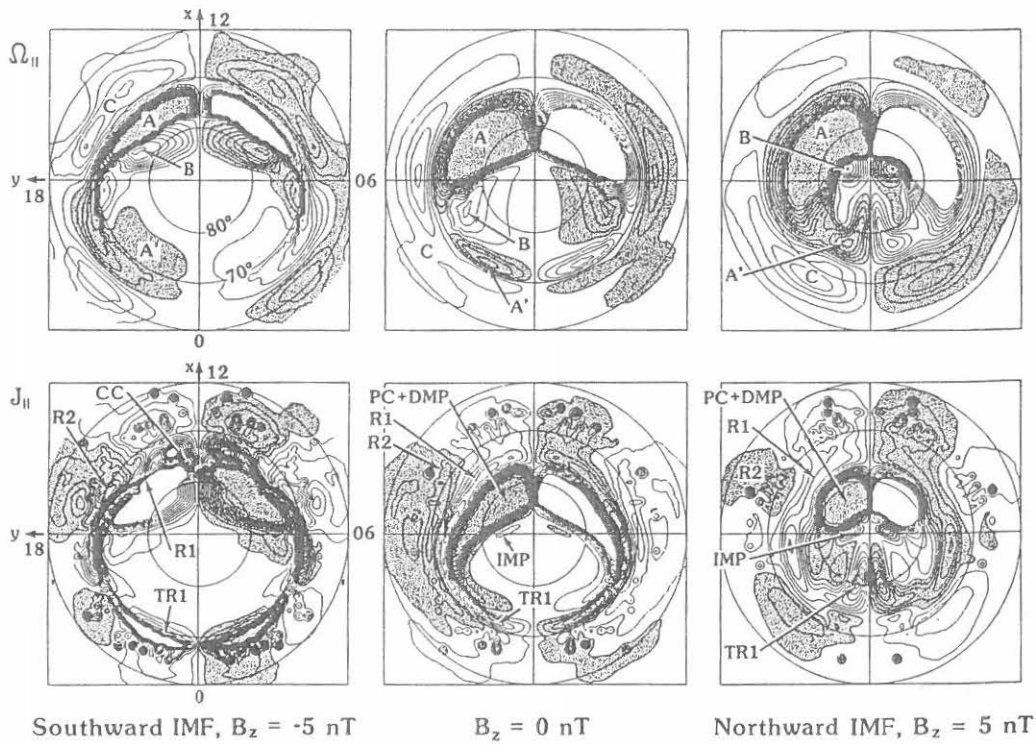

Fig. 3. Northern polar projections of the parallel vorticity, $\Omega_{\parallel}$ and the field aligned current, $J_{\parallel}$. The hatched areas correspond to positive $\Omega_{\parallel}$ and $J_{\parallel}$.

be clearly distinguished, and the earthward parallel flows appear in the dayside cusp and plasma sheet regions. The dayside cusp and plasma sheet are located at higher latitudes for northward IMF than for southward IMF. In particular the cusp latitude is about 82° for northward IMF (B_z = 5nT), 81° for no uniform IMF (B_z = 0nT) and 76° for southward IMF (B_z = -5nT). Moreover, the plasma sheet extends from midnight toward noon for northward IMF.

In Figure 3 the northern polar projections of the parallel vorticity, $\Omega_{\parallel}$, and the field aligned currents, $J_{\parallel}$, for the same three IMF conditions as Figure 2, are presented. Here $\Omega_{\parallel} = (\vec{\Omega} \cdot \vec{B})/B$, $J_{\parallel} = (\vec{J} \cdot \vec{B})/B$ and $\vec{\Omega} = \nabla \times \vec{v}$. The hatched areas correspond to positive $\Omega_{\parallel}$ and $J_{\parallel}$ (earthward field aligned current). In the parallel vorticity panel ($\Omega_{\parallel}$) there are four types of convection cells: viscous cells (A), tail lobe (or plasma sheet) cells (A'), high latitude (or merging) cells (B) and induced viscous cells (C) at low latitudes. There are also four major types of field aligned currents: region 1 currents (R1) at intermediate latitudes, tail region 1 currents (TR1) in the nightside, region 2 currents (R2) at low latitudes, and polar cap currents at high latitudes. The polar cap field aligned currents include dayside cusp currents (DC) for southward IMF and dayside magnetopause currents (DMP) and polar cap northern B_z currents (PC) for other cases. There is a small sign of inner magnetopause currents (IMP) in higher latitudes. The region 1 currents flow away from the ionosphere on the dusk side and flow into it on the dawn side, while the region 2 and polar cap currents flow into the ionosphere on the dusk side and flow out from it on the dawn side. It is important to note that the region 1 type currents expand into the polar cap for southward IMF. This occurred because the integration was carried out along open field lines which extend through the magnetosphere. When the integration is limited to the magnetosphere the region 1 currents are replaced with the cusp currents of region 2 type (see Ogino et al., 1986).

3.2 Simulation results for high spatial resolution

The magnetospheric configuration and polar cap structure will be demonstrated with typical simulation results from five different IMF conditions: (a) imposed southward IMF with $B_z = B_{zo}$ = -5nT, (b) incoming southward IMF with B_z = -5nT and B_{zo} = 0nT, (c) no IMF with $B_z = B_{zo}$ = 0nT, (d) incoming northward IMF with B_z = 5nT and B_{zo} = 0nT and (e) imposed northward IMF with $B_z = B_{zo}$ = 5nT, where B_z and B_{zo} stand for the z-component of IMF incoming with the upstream solar wind

and the z-component of IMF initially imposed in the whole system, respectively. Therefore, the essential difference between (a) and (b) for southward IMF is whether or not the uniform southward IMF is initially imposed inside the earth's magnetosphere. We used a (N_x, N_y, N_z) = (150, 50, 50) point grid with 0.5Re grid spacing as was previously mentioned. The snap shot shown in the following figures is depicted at 1280 time steps or 39 minutes for cases (a), (b) and (c), and at 1536 time steps or 48 minutes for (d) and (e).

In Figure 4 are shown the magnetospheric configuration and polar cap structure for case (a) with an imposed southward IMF of $B_z = B_{z0} = -5nT$. The upper panel shows the 3-dimensional configuration of the magnetic field lines where the green correspond to the closed field lines with both ends returning to the ionosphere, and the blue field lines are open with one end in the ionosphere and one connected to the interplanetary field. The yellow and red field lines are completely detached from the earth. The middle panel shows the northern polar projections of the plasma density ρ, plasma pressure p, parallel velocity $v_{\parallel}$, open-closed field region, parallel vorticity $\Omega_{\parallel}$ and field aligned current $J_{\parallel}$. Red and yellow represent positive values while blue means negative. For instance, in $v_{\parallel}$ the earthward flow is shown by the red areas and the tailward flow by the blue areas, while in the parallel current plot the earthward current is red and the upward current is blue. On the open-closed field region panel the closed magnetic field region is depicted in blue while the open field region is in red and yellow. Red indicates that the field line leaves the back ($x=x_0$) of the simulation box and yellow indicates that the field line leaves the top ($z=z_0$). The bottom panel left display shows cross sectional patterns of the magnetic field, plasma pressure and density in the noon-midnight meridional (x-z) and equatorial (x-y) planes and the tail cross sectional patterns (y-z plane) at two different positions in the tail ($x = -15R_e$ and $-30R_e$). Here red corresponds to the maximum.

For the imposed southward IMF in Figure 4, magnetic reconnection near the subsolar point and the formation of a near-earth magnetic neutral line are clearly seen. The tail neutral line which is initially located at $x = -19R_e$ moves towards the earth until about $x = -9R_e$. The plasma sheet is separated by tail magnetic reconnection at the near-earth neutral line, and its tailward part begins to propagate tailward as a plasmoid. One of the interesting features is that the plasma sheet and the plasmoid are extremely thin in the z direction over the wide ranges of the x and y directions. The feature can be

also seen on the tail cross-sectional pattern. On the northern polar projections the positions of the cusp and the plasma sheet are clearly recognized from p and $v_{\parallel}$. The cusp latitude is about 77° and the open region expands until 65° latitude at midnight. The viscous cells, tail lobe cells and induced viscous cells are seen on $\Omega_{\parallel}$. The pattern of field aligned currents has a fine structure in comparison with that in Figure 3, however, a large-scale pattern composed of region 1, region 2 and tail region 1 currents does not change much. The cusp currents appear in the dayside polar cap and in higher latitudes than the region 1 currents. In this case we limited the integration to the region within the magnetosphere (region for $v_x > -0.2\ v_{sw}$). The cusp currents are located in the open field region, so they must be generated by a strong twisting of reconnected open field lines near the dayside magnetopause.

In Figure 5 the magnetospheric configuration and polar cap structure for case (b) with an incoming southward IMF of B_z = -5nT and B_{zo} = 0nT have been plotted. In this case the tail neutral lines are not yet formed 39 minutes after the simulation begins, although dayside reconnection is occurring. The tail magnetic field lines change from dipolar to concave at x = $-10R_e$. The plasma sheet is thicker than it was for case (a). On the polar projections, the cusp shifts to a somewhat higher latitude of 80°, and the open field region shrinks considerably. It is noted that a narrow arch of the high plasma pressure is formed at 75° latitude in the dayside. In the same region an earthward flow and field aligned currents are enhanced. These phenomena seem to be associated with a strong distortion of the geomagnetic field lines inside the magnetopause.

In Figure 6 we present the magnetospheric configuration and polar cap structure for case (c) with no IMF ($B_z = B_{zo}$ = 0nT). In this case reconnected open field lines are not seen in the dayside magnetosphere although there are distorted closed field lines near the magnetopause. The plasma sheet becomes thicker in the z direction near the noon-midnight meridian. On the polar plots, the open field region shifts to a higher latitude of 82° at noon, although it extends to almost the same latitude as in case (b) at midnight. Note the field lines are open, even though the IMF is zero because they exit the rear ($x=x_o$) of the simulation box. The cusp latitude is about 80° at noon. The cusp currents noted in cases (a) and (b) disappear, and the dayside magnetopause currents with the region 2 sense are seen at the highest latitudes.

In Figure 7 the magnetospheric configuration and polar cap

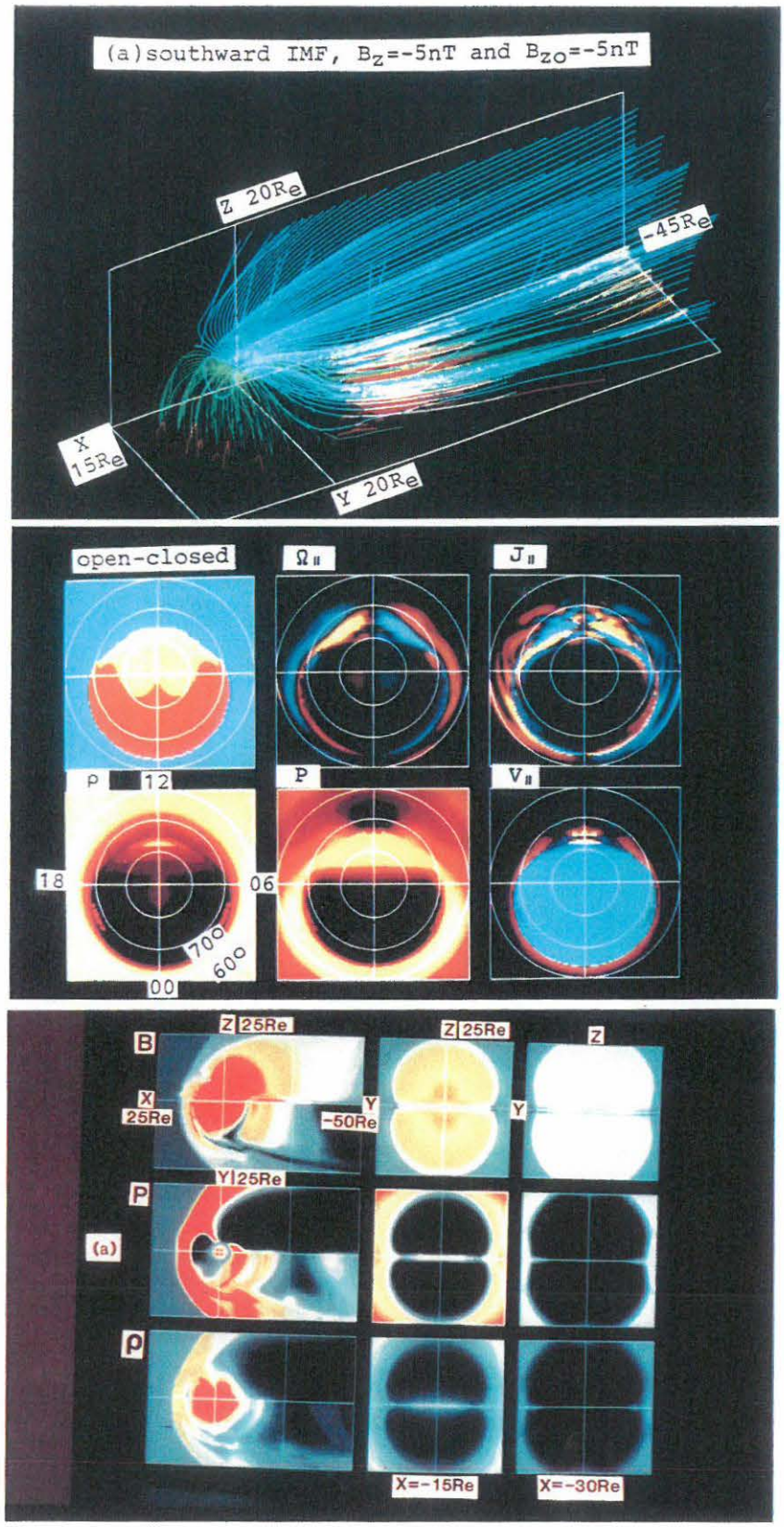

Fig. 4. The magnetospheric configuration and polar cap structure for case (a) with an imposed southward IMF of B_z=B_{zo}=-5nT.

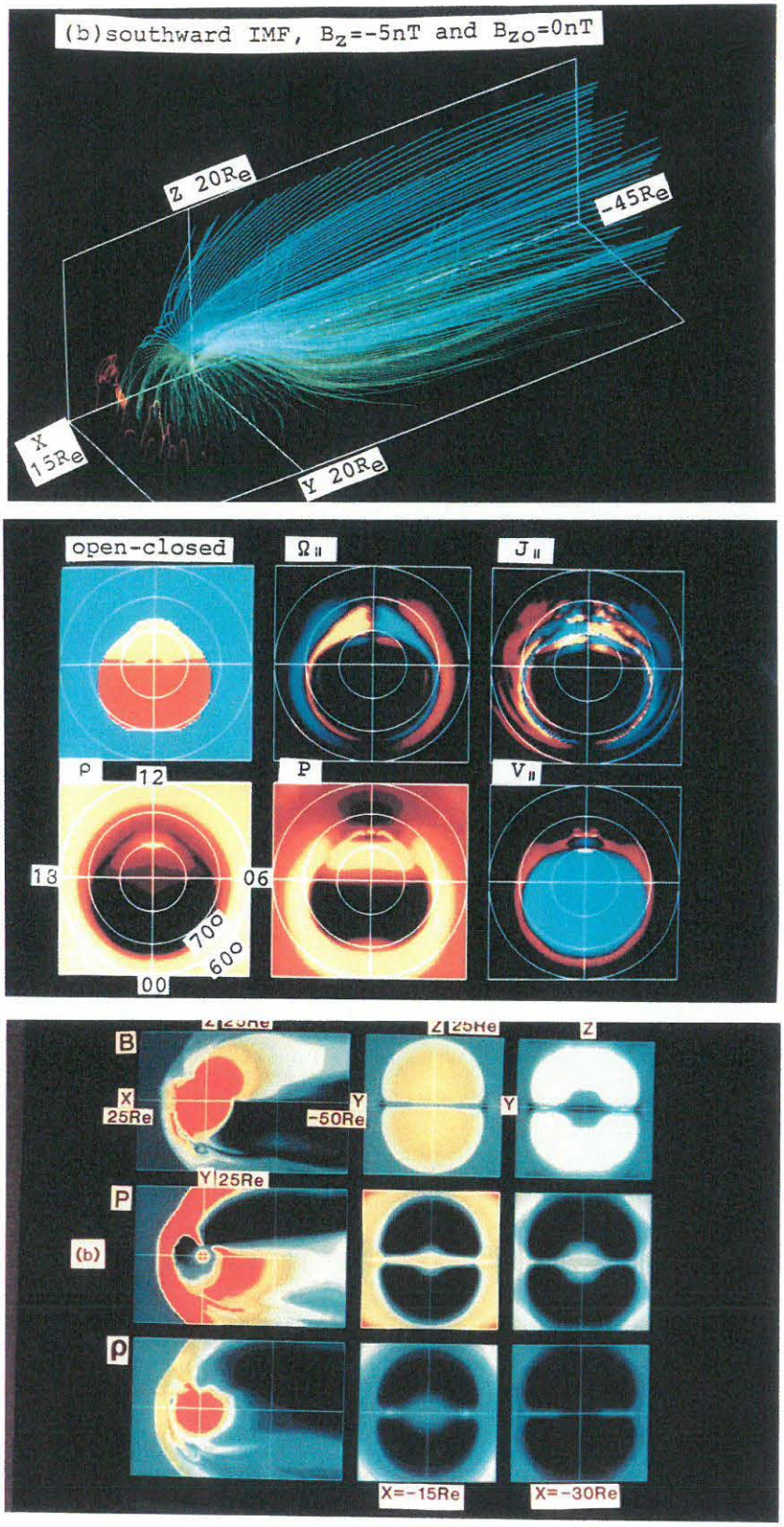

Fig. 5. The magnetospheric configuration and polar cap structure for case (b) with an incoming southward IMF of B_z=-5nT and B_{zo}=0nT.

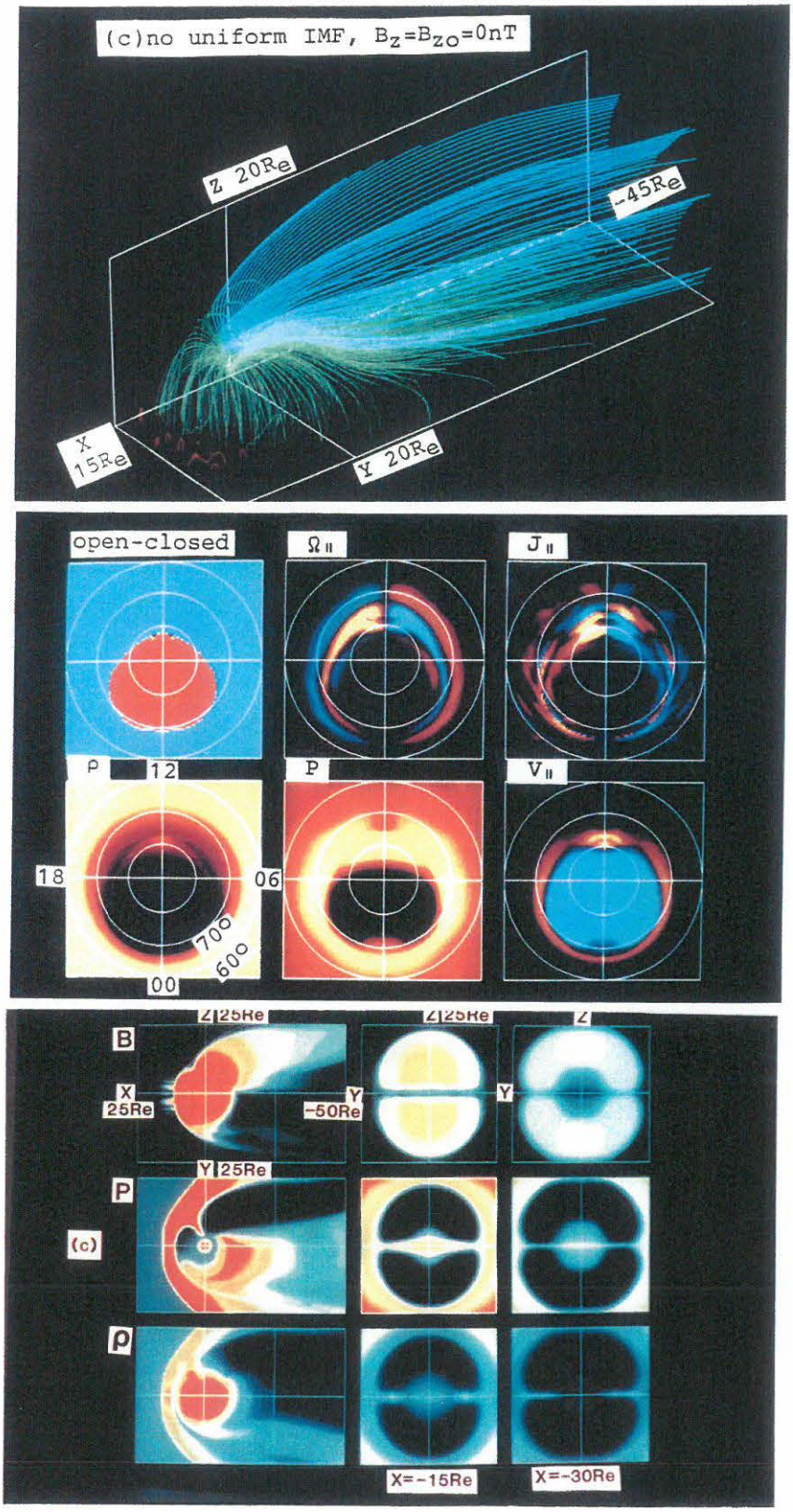

Fig. 6. The magnetospheric configuration and polar cap structure for case (c) with no IMF.

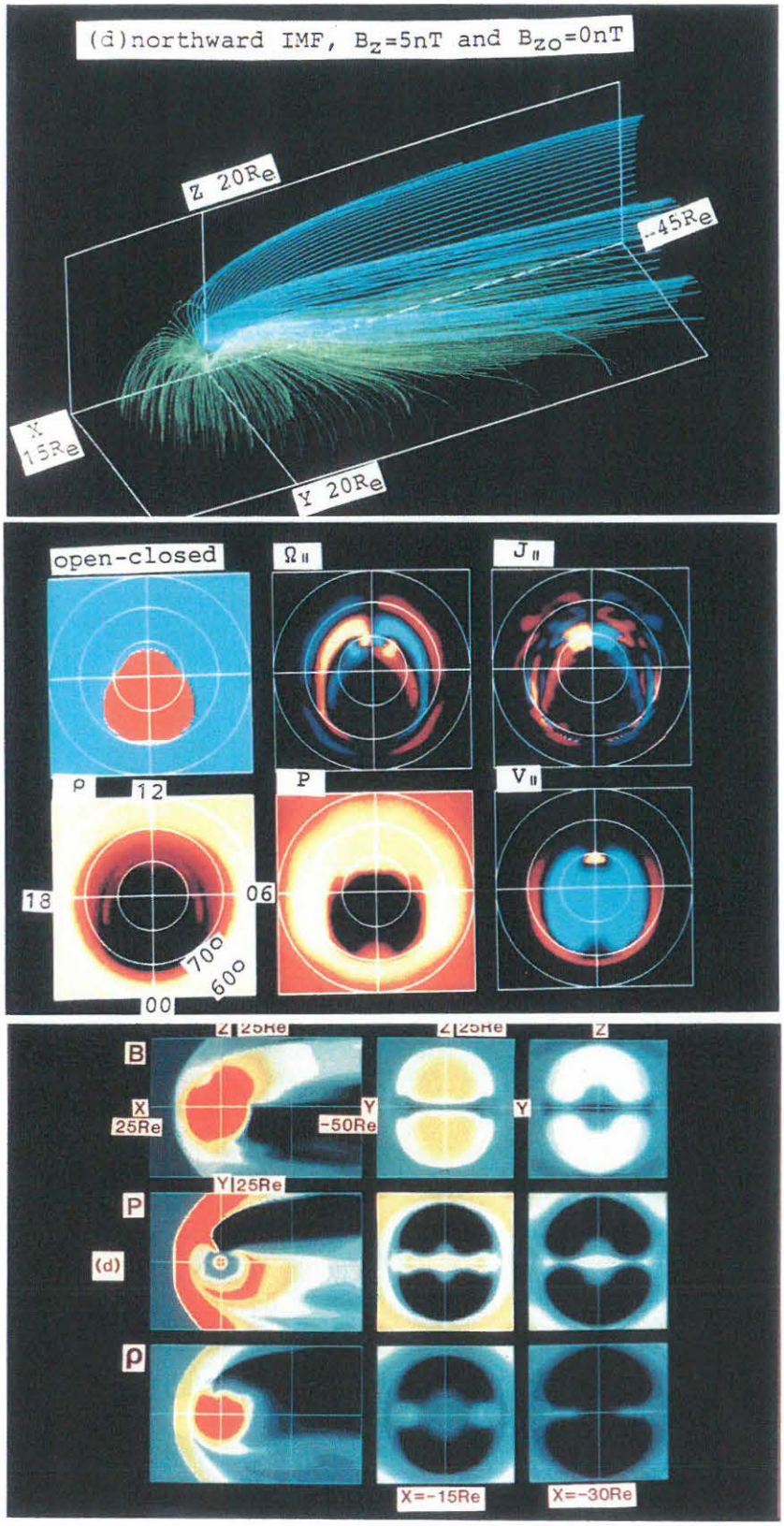

Fig. 7. The magnetospheric configuration and polar cap structure for case (d) with an incoming northward IMF of B_z=5nT and B_{zo}=0nT.

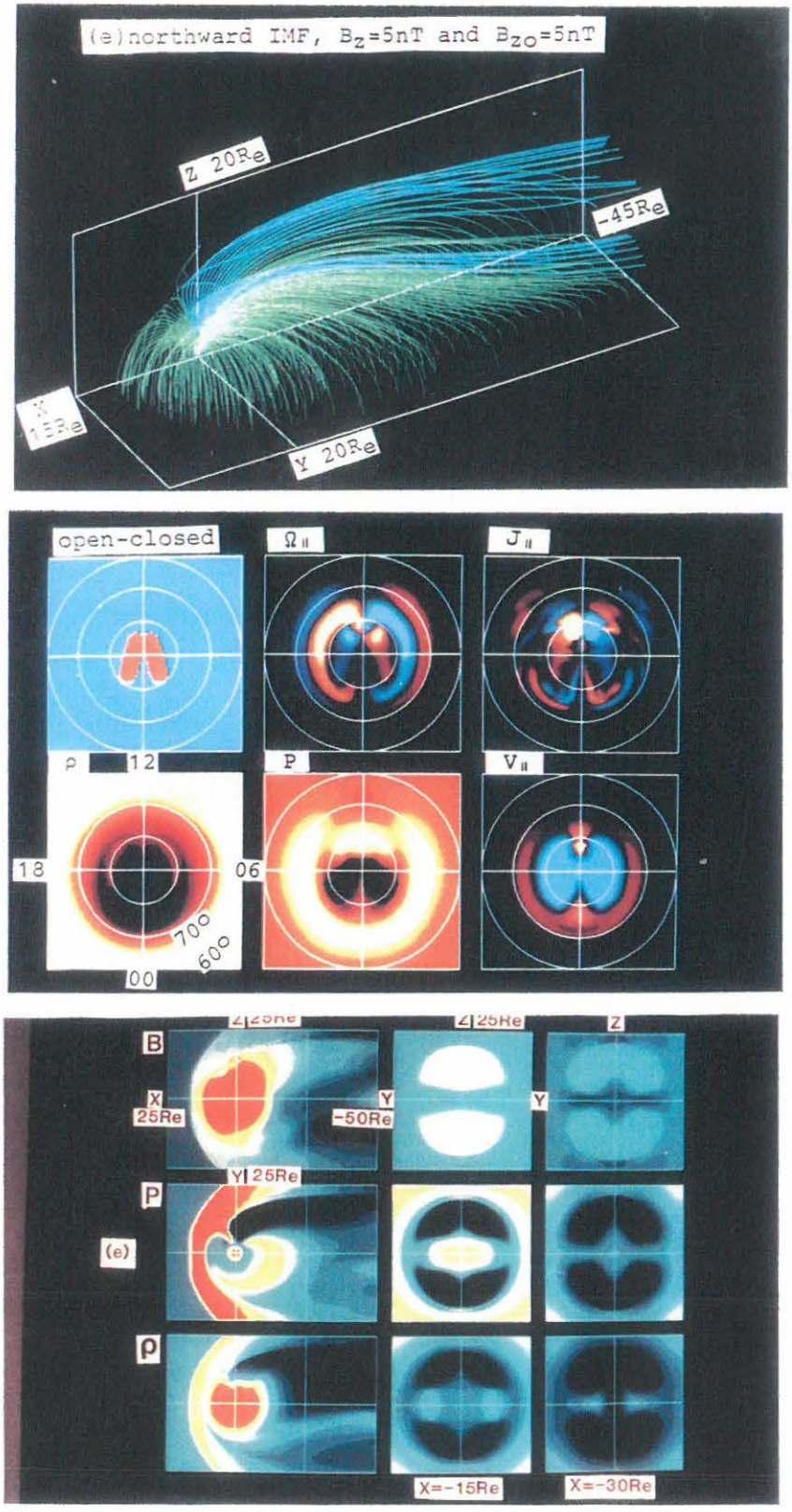

Fig. 8. The magnetospheric configuration and polar cap structure for case (e) with an imposed northward IMF of $B_z=B_{zo}=5$nT.

structure for case (d) with an incoming northward IMF of B_z = 5nT and B_{z0} = 0nT have been plotted. In this case the closed field lines, which extend toward the high latitude tail over the cusp are seen. They are evidence that magnetic reconnection is occurring in the high latitude tail. The region of the dipolar geomagnetic field lines expands, that is the tail field lines become rather convex. At the same time the plasma sheet expands toward the lobes and the high latitude ionosphere. On the polar plots, the high latitude or merging convection cells appear, and the northern B_z polar cap field aligned currents are enhanced. The high latitude convection is consistent with sunward convection near the noon-midnight meridian and is produced from the high latitude tail reconnection. The plasma sheet extension is slightly more pronounced than it was for case (c).

In Figure 8 we plot the magnetospheric configuration and polar cap structure for case (e) with an imposed northward IMF of $B_z = B_{z0}$ = 5nT. Again magnetic field lines reconnect in the high latitude tail. Convex field lines are formed near the noon-midnight meridian in the magnetotail. As a result the plasma sheet thickens near the noon-midnight meridian in the tail and also expands towards the higher latitude ionosphere near the earth. On the polar plots the open field region shrinks greatly. The plasma sheet extends as a narrow finger from midnight toward noon. The region of the plasma sheet extension corresponds to a closed field region, and field aligned currents of the region 1 type are generated on both sides of the plasma sheet extension.

5. Discussion

The quasi-steady state magnetospheric configuration and polar cap structure for five different IMF conditions have been calculated by using a 3-dimensional time-dependent MHD model with high spatial resolution ($\Delta x=0.5R_e$) and longer magnetotail ($x=-50.25R_e$). The high resolution model reproduced results from an earlier model [Ogino and Walker, 1984; Ogino et al., 1985; 1986] which had lower spatial resolution ($\Delta x=1R_e$) and a shorter magnetotail ($x=-30.5R_e$). The main difference between the two models is the fine structure.

In Figure 9 we have plotted the 3-dimensional configurations of field aligned currents in the earth's magnetosphere as a function of the z-components of IMF. There are three kinds of field aligned currents in the ionosphere: dayside cusp (CC) or polar cap (PC)

current at the highest latitudes, region 1 currents (R1) at middle latitudes, and region 2 currents (R2) at the lowest latitudes [Iijima and Potemra, 1976a; 1976b; Iijima et al., 1984]. On the dusk side the polar cap (PC or CC) and R2 currents flow into the ionosphere whereas the R1 current flows away from the ionosphere. In the magnetotail there are fundamentally four kinds of field aligned currents. Starting from the high latitude tail and moving towards the plasma sheet, they are the dayside magnetopause (DMP), inner magnetopause (IMP), polar cap (PC or CC) and tail region 1 (TR1) currents. The DMP current is partly replaced with the southern B_z magnetopause current (SMP) for southward IMF. The DMP current partly flows into the IMP and the polar cap (PC or CC) currents in the polar region inside the magnetopause. Near the equator the R1 current primarily merges into the cross tail current in the plasma sheet and partly flows into the R2 current. The TR1 current merges into the cross tail current in the far tail and then connects with the magnetopause currents.

It should be noted that the types of field aligned currents obtained in the polar cap or the magnetotail do not depend on the IMF B_z component. However, the spatial distributions of currents are greatly affected by the IMF. The field aligned currents are earthward at high latitudes (PC or CC) and at low latitudes (R2) on the dusk side, while they are upward at middle latitudes (R1 and TR1). The

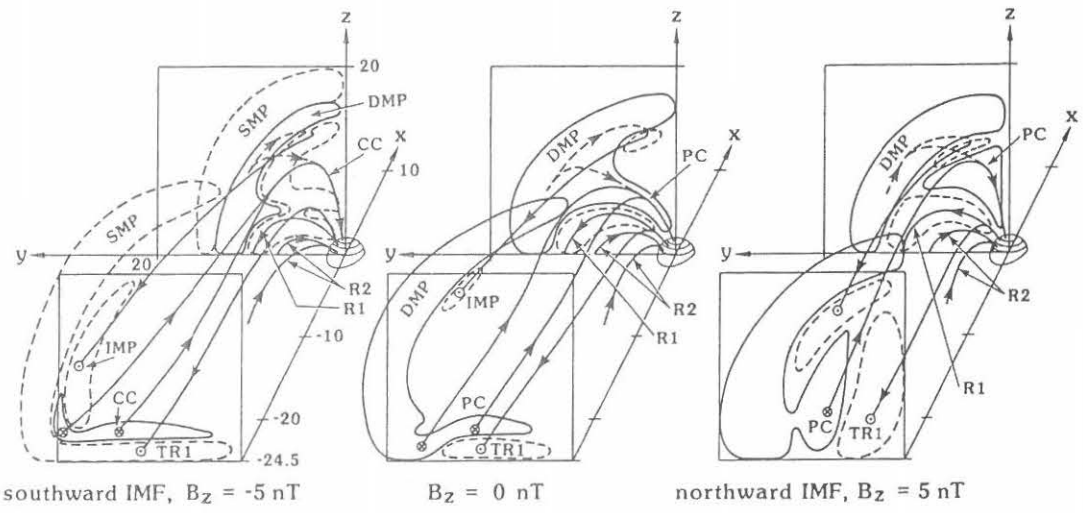

Fig. 9. Three-dimensional configuration of the field aligned currents in the earth's magnetosphere as a function of the z-component of the IMF.

field aligned currents in the magnetotail are tailward near the equator (TR1) and earthward near the lobe and magnetopause (PC or CC). The field aligned currents flow in the opposite directions on the dawn side. Moreover, the tail region 1 (TR1) currents are parallel to the equator for southward IMF but extend along the noon-midnight meridian for northward IMF. This phenomenon corresponds to the appearance of region 1 type field aligned currents on both sides of the plasma sheet extension for northward IMF and also is consistent with observation of the theta aurora [Frank et al., 1982; Frank et al., 1986; Menietti and Burch, 1987].

The field aligned currents can be generated either by the parallel vorticity or by pressure gradients [Hasegawa and Sato, 1979; Stern, 1983; Vasyliunas, 1984; Ogino, 1986]. The relationships are approximately described by the followig coupled equations [Ogino, 1986],

$$\frac{d\Omega_{\parallel}}{dt} - \frac{\mu}{\rho}\nabla^2\Omega_{\parallel} - \frac{B^2}{\rho}\nabla_{\parallel}\frac{J_{\parallel}}{B} = -\frac{2\vec{B}\cdot\nabla p \times \vec{\nabla}B}{\rho B^2} \qquad (2a)$$

$$\frac{\partial J_{\parallel}}{\partial t} - \frac{\eta}{\mu_0}\nabla^2 J_{\parallel} - \frac{1}{\mu_0}\nabla_{\parallel} B\Omega_{\parallel} = 0, \qquad (2b)$$

where $\nabla_{\parallel} = (\vec{B}/B)\cdot\vec{\nabla}$ and μ_0 is the magnetic permeability. When there are no viscosity and resistivity, the coupled equations are reduced to $\nabla_{\parallel}(J_{\parallel}/B) = 2\vec{B}\cdot\nabla p \times \vec{\nabla}B/B^4$ in a steady state and to $J_{\parallel} = \pm(\rho/\mu_0)^{1/2}\Omega_{\parallel}$ for the Alfven mode without pressure gradients. Thus it can be understood that the parallel vorticity and the gradient of plasma pressure are primarily two important quantities for the generation of field aligned currents. In the present simulation the region 1 currents are mainly generated from the magnetospheric convection and the region 2 currents from the pressure gradients at the inner boundary of the plasma sheet.

The generation mechanisms of the region 1 and 2 field aligned currents have been discussed in detail by the previous simulation results [Ogino, 1986; Ogino et al., 1985; 1986]. The tail region 1 currents flow at the boundary layers between the lobes and the plasma sheet, and are probably generated by both the lobe convection and the pressure gradients. The cusp currents for southward IMF come from the parallel vorticity caused by the strong twisting of reconnected open field lines, while the northern B_z polar cap currents come from the parallel vorticity of the sunward convection due to high latitude tail

reconnection. The cusp currents and the northern B_z currents at highest latitudes flow in the same directions, although the polar convection near the sun-earth meridian is opposite, that is, antisunward for southward IMF and sunward for northward IMF. This is because the cusp currents and the northern B_z currents are generated by the parallel vorticities in association with open and closed field lines, respectively.

Next, the effect of the IMF B_z component will be discussed in more detail. In general the polar cap or open field region expands for southward IMF while it shrinks for northward IMF. There are also differences which depend on the initial conditions in the simulation. For example, if we compare the case of an imposed southward IMF with that of an incoming IMF, we find that the lower edge of the open field region on the polar projection does not change so much at noon, it somewhat expands toward the low latitudes on the dawn and dusk sides and shifts toward the low latitudes near midnight. Moreover, the large scale convection patterns and parallel current patterns in the dayside polar cap are very similar in the two cases. Thus the main differences between the imposed IMF and incoming IMF appear in the magnetotail in the plasma sheet region and are relatively small in the dayside magnetosphere. This suggests two possibilities in the present MHD model. First, the magnetosphere either needs a longer time than about 40 minutes for the IMF B_z component to penetrate into the magnetotail or only an amount of IMF B_z component can penetrate in the magnetotail in a steady state. In this calculation the magnetotail was only $50R_e$ long. It is important to include a more distant magnetotail in our simulation system. The shortness of the tail is one reason why a near-earth magnetic neutral line did not form after 39 minutes in the incoming southward IMF case and why the plasma sheet extension is less pronounced for the incoming northward IMF case. In further studies we will examine how quickly the IMF B_z component penetrates into the magnetotail and the amount of IMF B_z component that can penetrate into the magnetotail in a steady state.

The boundary condition near the earth is fixed at $3.5R_e$, and all the perturbations are artificialy damped to zero through a smooth transition layer for $3.5\ R_e < r \leq 5.5$ Re. Therefore, the field aligned currents do not form a closed loop in the ionosphere. Rather they close just outside of the model ionosphere. However, since the field aligned currents which flow toward the ionosphere or toward the outer magnetosphere steadily exist for $r > 3.5\ R_e$, it is expected that they can be stretched up to the ionosphere with no artificial damping and

with higher spatial resolution near the earth. Moreover, the characteristic features of field aligned currents are self-consistently calculated in the generation regions of the earth's magnetosphere and represent a similar polar pattern to the observations depending on the z-component of IMF. It is, of course, an important future problem to include the response of ionosphere in the present global MHD model.

6. Conclusion

The IMF B_z dependent interaction between the solar wind and the earth's magnetosphere has been studied by using a high-resolution and time-dependent three-dimensional MHD model. The characteristic features of the earth's magnetosphere, such as bow shock, magnetosheath, magnetopause, magnetotail, and plasma sheet, have been modeled for five different IMF conditions.

The four major convection cells composed of viscous cells, tail lobe cells, high latitude merging cells and low latitude induced viscous cells. The four types of major field aligned currents composed of region 1 currents, tail region 1 currents, polar cap (or cusp) currents and region 2 currents, which were found in the low resolution model, were reproduced by the high resolution MHD model, although an additional fine structure also appeared. The open field region expands toward low latitudes in the nightside polar cap when the southward IMF is imposed rather than incoming. Also, the near-earth neutral line forms only for the imposed southward IMF case. Thus the effect of the IMF B_z component appears in the dayside magnetosphere after only about 10 minutes however it needs a longer time for the magnetotail.

For northward IMF the sunward convection near the noon-midnight meridian is similarly formed in both the imposed and incoming cases by the high latitude tail reconnection. However, the plasma sheet extension becomes less pronounced for incoming northward IMF, though it still continues to grow. Moreover, the open field region remarkably shrinks near midnight on the polar projection for imposed northward IMF.

In order to study the interaction between the solar wind, the magnetosphere and the ionosphere in more detail, we will need to include a realistic ionospheric model and possibly a magnetic diffusion term in the magnetotail. We also need to move the tail

boundary further and further away from the earth. Finally, we need to consider the dynamic behavior of the earth's magnetosphere.

Acknowledgements

This work was supported by a Grant-in-Aid for Science Research from the Ministry of Education, Science and Culture, and by the NASA Solar Terrestrial Theory Program Grant NAGW-78. The simulations were performed at the Computer Center of Institute of Plasma Physics, Nagoya University, the Computer Center of Nagoya University and the Computer Center of the Institute of Space and Astronautical Science.

References

Brecht, S.H., J.G. Lyon, J.A. Fedder, and K. Hain, A simulation study of east-west IMF effects on the magnetosphere, **Geophys. Res. Lett.**, **8**, 397-400, 1981.

Brecht, S.H., J.G. Lyon, J.A. Fedder, and K. Hain, A time dependent three-dimensional simulation of the earth's magnetosphere: Reconnection events, **J. Geophys. Res.**, **87**, 6098-6108, 1982.

Fedder, J.A., and J.G. Lyon, The solar wind-magnetosphere-ionosphere current-voltage relationship, **Geophys. Res. Lett.**, **14**, 880-883, 1987.

Frank, L.A., J.D. Craven, J.L. Burch, and J.D. Winningham, Polar views of the Earth's aurora with Dynamics Explorer, **Geophys. Res. Lett.**, **9**, 1001-1004, 1982.

Frank, L.A., J.D. Craven, D.A. Gurnett, S.D. Shawhan, D.R. Weimer, J.L. Burch, J.D. Winningham, C.R. Chappell, J.H. Waite, R.A. Heelis, N.C. Maynard, M. Sugiura, W.K. Peterson, and E.G. Shelly, The theta aurora, **J. Geophys. Res.**, **91**, 3177-3224, 1986.

Hasegawa, A., and T. Sato, Generation of field-aligned currents during substorm, in Dynamics of the Magnetosphere, edited by S.-I. Akasofu, pp. 529-542, D. Reidel, Hingham, Mass., 1979.

Iijima, T., and T.A. Potemra, The amplitude distribution of field-aligned current at northern high latitudes observed by TRIAD, **J. Geophys. Res.**, **81**, 2165-2174, 1976a.

Iijima, T., and T.A. Potemra, Field-aligned current in the dayside cusp observed by TRIAD, **J. Geophys. Res.**, **81**, 5971-5979, 1976b.

Iijima, T., T.A. Potemra, L.J. Zanetti, and P.F. Bythrow, Large-scale

Birkeland currents in the dayside polar region during strongly northward IMF-A new Birkeland current system, **J. Geophys. Res.**, **89**, 7441-7452, 1984.

Leboeuf, J.N., T. Tajima, C.F. Kennel, and J.M. Dawson, Global simulations of the time-dependent magnetosphere, **Geophys. Res. Lett.**, **5**, 609-612, 1978.

Leboeuf, J.N., T. Tajima, C.F. Kennel, and J.M. Dawson, Global simulations of the three-dimensional magnetosphere, **Geophys. Res. Lett.**, **8**, 257-260, 1981.

Lyon, J.G., S.H. Brecht, J.A. Fedder, and P.J. Palmadesso, The effect on the earth's magnetotail from shocks in the solar wind, **Geophys. Res. Lett.**, **7**, 721-724, 1980.

Lyon, J.G., S.H. Brecht, J.D. Huba, J.A. Fedder, and P.J. Palmadesso, Computer simulation of a geomagnetic substorm, **Phys. Rev. Lett.**, **46**, 1038-1041, 1981.

Lyon, J.G., J.A. Fedder, and J.D. Huba, The effects of different resistivity models on magnetotail dynamics, **J. Geophys. Res.**, **91**, 8057-8064, 1986.

Menietti, J.D., and J.L. Burch, DE 1 observations of theta aurora plasma source regions and Birkeland current change carriers, **J. Geophys. Res.**, **92**, 7503-7518, 1987.

Ogino, T., and R.J., Walker, A magnetohydrodynamic simulation of the bifurcation of tail lobes during intervals with a northward interplanetary magnetic field, **Geophys. Res. Lett.**, **11**, 1018-1021, 1984.

Ogino, T., A three dimensional MHD simulation of the interaction of the solar wind with the earth's magnetosphere: The generation of field-aligned currents, **J. Geophys. Res.**, **91**, 6791-6806, 1986.

Ogino, T., R.J. Walker, M. Ashour-Abdalla, and J.M. Dawson, An MHD simulation of B_y-dependent magnetospheric convection and field-aligned currents during northward IMF, **J. Geophys. Res.**, **90**, 10835-10842, 1985.

Ogino, T., R.J., Walker, M. Ashour-Abdalla, and J.M. Dawson, An MHD simulation of the effects of the interplanetary magnetic field B_y component on the interaction of the solar wind with the earth's magnetosphere during southward IMF, **J. Geophys. Res.**, **91**, 10029-10045, 1986.

Stern, D.P., The origins of Birkeland currents, **Rev. Geophys.**, **21**, 125-138, 1983.

Vasyliunas, V.M., Fundamentals of current description, in Magnetospheric Currents, Geophys. Monogr. Ser., vol. 28, edited

by T.A. Potemra, pp. 63-66, AGU, Washington, D.C., 1984.

Walker, R.J. and T. Ogino, Field aligned currents and magnetospheric convection: A comparison between MHD simulations and observations, **Proceedings of the Huntsville Workshop on Magnetosphere-Ionosphere Plasma Models**, D. Reidel, 1987.

Wu, C.C., R.J. Walker, and J.M. Dawson, A three-dimensional MHD model of the earth's magnetosphere, **Geophys. Res. Lett.**, **8**, 523-526, 1981.

Wu, C.C., Shape of the magnetosphere, **Geophys. Res. Lett.**, **10**, 545-548, 1983.

Wu, C.C., The effects of dipole tilt on the structure of the magnetosphere, **J. Geophys. Res.**, **89**, 11048-11052, 1984.